PERGAMON International Journal of Engineering Science 38 (2000) 1303–1314

International Journal of Engineering Science

www.elsevier.com/locate/ijengsci

Flow and mass transfer on a stretching sheet with a magnetic field and chemically reactive species

H.S. Takhar [a,*], A.J. Chamkha [b], G. Nath [c]

[a] *School of Engineering, University of Manchester, Manchester M13 9PL, UK*
[b] *Department of Mechanical Engineering, Kuwait University, Safat, Kuwait*
[c] *Department of Mathematics, Indian Institute of Science, Bangalore-560012, India*

Received 30 April 1999; accepted 21 June 1999

(Communicated by E.S. ŞUHUBİ)

Abstract

An analysis has been carried out to obtain the flow and mass transfer characteristics of a viscous electrically conducting fluid on a continuously stretching surface with non-zero slot velocity. The motion is caused solely by the stretching surface which introduces non-similarity in the velocity and concentration fields. The partial differential equations governing the boundary layer flow and mass transfer are solved by using an implicit finite-difference scheme. The magnetic field significantly increases the surface skin friction, but slightly reduces the surface mass transfer. The surface mass transfer strongly depends on the Schmidt number and the reaction rate and it increases with their increasing values. The surface mass transfer for the first-order reaction is more than that for the second- or-third-order reaction.

1. Introduction

The heat, mass and momentum transport on a continuously moving or stretching sheet has several applications in, electro-chemistry and polymer processing [1–4]. Most of the studies deal with flow induced by surfaces moving with a constant velocity. Crane [5] first studied the flow caused by an elastic sheet whose velocity varies linearly with the distance from a fixed point on the sheet. Since then, the flow, heat and mass transfer problem with or without suction (blowing) or magnetic field has been considered by several investigators [6–13], who obtained self-similar

* Corresponding author. Tel.: +44-161-275-4356; fax: +44-161-275-4361.
E-mail address: hstakhar@fs1.eng.man.ac.uk (H.S. Takhar).

0020-7225/00/$ - see front matter
PII: S0020-7225(99)00079-8

solutions. It may be remarked that the assumption of linear variation of the surface velocity with the distance ($u_w = ax$) gives the unrealistic surface velocity at $x = 0$, to be zero. Jeng et al. [14] considered the non-similar flow where the velocity of the stretching sheet is $u_w = u_0(1 + x/L)$. Also, the self-similarity is destroyed by the presence of a chemical reaction in the mass diffusion equation except in the case of a stagnation-point flow [15]. Recently, Andersson et al. [15] have investigated the transport of mass and momentum of chemically reactive species in the laminar flow over a linearly stretching surface and solved the nonlinear ordinary differential equations governing the self-similar flow.

In this study, we have investigated the flow and mass diffusion of chemical species with first and higher order reactions over a continuously stretching sheet with an applied magnetic field. The velocity of the surface varies linearly with the distance x with non-zero velocity at $x = 0$ ($u_w = u_0(1 + x/L)$). The reactive component resulting from the stretching surface undergoes an isothermal and homogeneous one-stage reaction as it diffuses into the surrounding fluid. The nonlinear partial differential equations governing the non-similar flow and mass transfer are solved numerically using an implicit finite-difference scheme. The particular cases of the present results are compared with those of Jeng et al. [14] and Andersson et al. [15].

2. Problem formulation

Let us consider the steady incompressible flow of a viscous electrically conducting fluid over a stretching sheet (surface) with a magnetic field **B** which is applied normal to the surface. The physical system to be investigated is given in the inset of Fig. 1. We use the Cartesian x–y coordinate system which is fixed in space and at $x = y = 0$ a thin solid surface is extruded which moves in the x-direction with surface velocity $u_w = u_0(1 + x/L)$. This introduces non-similarity in the equations. The motion in an otherwise quiescent fluid is caused by the stretching surface. The concentration of the reactant is maintained at a constant value C_w at the sheet and is assumed to vanish far away from the sheet. It is further assumed that the magnetic Reynolds number $Rm = \mu_0 \sigma VL \ll 1$, where μ_0 is the magnetic permeability, σ the electrical conductivity and V and L are the characteristic velocity and length, respectively. Under this condition we can neglect the effect of the induced magnetic field in comparison to the applied magnetic field. The electrical current flowing in the fluid will give rise to the induced magnetic field if the fluid were an electrical insulator, but here we have taken the fluid to be electrically conducting. Hence only the applied magnetic field plays a role and gives rise to the magnetic force $F_x = \sigma B^2 u/\rho$, where ρ is the density of the fluid. Under the above assumptions the boundary layer equations governing the flow and concentration fields are given by [14–16]:

$$u_x + v_y = 0, \tag{1}$$

$$uu_x + vu_y = vu_{yy} - \sigma B^2 u/\rho, \tag{2}$$

$$uC_x + vC_y = DC_{yy} - K_0 C^N. \tag{3}$$

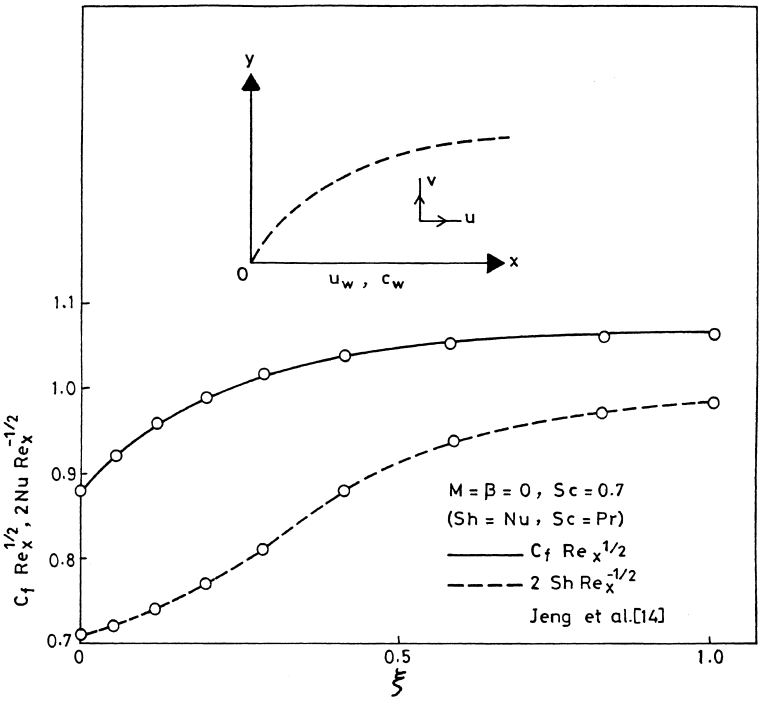

Fig. 1. Comparison of skin friction and mass (heat) transfer coefficients ($C_f\ Re_x^{1/2}, -2\ Sh\ Re_x^{-1/2}$).

The boundary conditions can be expressed as:

$$\begin{aligned} &u(x,0) = u_w = u_0(1 + x/L), \quad \upsilon(x,0) = 0, \quad C(x,0) = C_w, \\ &u(x,\infty) = C(x,\infty) = 0, \\ &u(0,y) = C(0,y) = 0, \quad y > 0 \end{aligned} \tag{4}$$

Here x and y are, respectively, the distances along and perpendicular to the surface; u and v are the components of the velocity along x and y directions, respectively; v is the kinematic viscosity, C the concentration; D the molecular diffusion coefficient; K_0 the reaction rate constant; N is a constant which denotes the order of reaction; u_w the surface velocity at a distance x and u_0 is its value at $x = 0$; the subscript w denotes condition at the surface; and the subscripts x and y denote derivatives with respect to x and y, respectively.

In order to make the above equations dimensionless, we apply the transformations

$$\begin{aligned} &\eta = (2\overline{\xi}v)^{-1/2}y, \quad \overline{\xi} = \int_0^x u_w(x)\,\mathrm{d}x, \quad \Psi(x,y) = (2v\overline{\xi})^{1/2} f(\overline{\xi},\eta), \\ &u = \partial\Psi/\partial y = u_w\, f'(\overline{\xi},\eta), \quad v = -\partial\Psi/\partial x = -(2\overline{\xi}v)^{1/2}(u_w/2\overline{\xi})[f \\ &\qquad + 2\overline{\xi}\, f_{\overline{\xi}} + (\lambda - 1)\eta f'], \quad g(\overline{\xi},\eta) = C/C_w, \ M = \sigma B^2 L^2/\mu, \xi = x/L, \\ &u_w = u_0(1 + \xi), \quad \overline{\xi} = u_0 L\ \xi(1 + \xi/2), \quad Sc = v/D, \quad \beta = K_0 L (C_w)^{N-1} \end{aligned} \tag{5}$$

to Eqs. (1)–(3) and we find that Eq. (1) is identically satisfied and Eqs. (2) and (3) reduce to

$$f''' + ff'' - \lambda f'\, f' - \lambda_1\, Mf' = \lambda_2 \xi (f'\, f'_\xi - f''\, f'_\xi), \tag{6}$$

$$Sc^{-1}\, g'' + fg' - \beta \lambda_3 g^N = \lambda_2 \xi (f' g_\xi - g'\, f_\xi). \tag{7}$$

The boundary conditions (4) can be rewritten as

$$\begin{aligned} &f(\xi,0) = 0, \quad f'(\xi,0) = g(\xi,0) = 1, \\ &f'(\xi,\infty) = g(\xi,\infty) = 0, \end{aligned} \tag{8}$$

where

$$\begin{aligned} &\lambda = (2\overline{\xi}/u_w)(\mathrm{d}u_w/\mathrm{d}\overline{\xi}) = 2\xi(1+\xi/2)(1+\xi)^{-2} \\ &\lambda_1 = (2\overline{\xi}/u_w^2)(u_0/L)(x/L) = 2\xi(1+\xi/2)(1+\xi)^{-2}, \\ &\lambda_2 = 2(1+\xi/2)(1+\xi)^{-1}, \quad \lambda_3 = 2\overline{\xi}/(u_w L) = 2\xi(1+\xi/2)(1+\xi)^{-1}, \\ &2\overline{\xi}\partial/\partial\overline{\xi} = \lambda_2 \xi \partial/\partial\xi. \end{aligned} \tag{9}$$

Here $\overline{\xi}$, η are the transformed coordinates; ψ and f are the dimensional and dimensionless stream functions, respectively; ξ is the distance along the surface; M the magnetic parameter; Sc the Schmidt number; g the dimensionless concentration; f' the dimensionless velocity along the surface; β the dimensionless reaction rate parameter; λ, λ_1, λ_2 and λ_3 are the dimensionless functions of ξ; and prime denotes the derivative with respect to η; and the subscript ξ denotes the derivative with respect to ξ.

It may be noted that Eqs. (6) and (7) for $M = 0$ (no magnetic field) and $\beta = 0$ (without chemical reaction) reduce to those of Jeng et al. [14] if we replace Sc by Pr, where Pr is the Prandtl number. Also, Eqs. (6) and (7) for $M = \xi = 0, \lambda = \lambda_3 = 1$ reduce to those of Andersson et al. [15].

The surface skin friction coefficient C_f can be expressed as

$$C_\mathrm{f} = -2\mu(\partial u/\partial y)_{y=0}/\rho u_w^2 = -2^{-1/2}\, Re_x^{-1/2}(1+\xi/2)^{-1/2} f''(\xi,0). \tag{10a}$$

Similarly, the mass transfer coefficient in terms of the Sherwood number Sh is given by

$$Sh = -x(\partial C/\partial y)_{y=0}/C_w = -2^{-1/2}\, Re_x^{1/2}(1+\xi)(1+\xi/2)^{-1/2} g'(\xi,0), \tag{10b}$$

where $Re_x = u_0 x/v$ is the local Reynolds number and μ is the coefficient of dynamic viscosity.

3. Method of solution

The partial differential equations (6) and (7) under conditions (8) are solved numerically by an implicit, iterative tridigonal finite-difference method similar to that of Blottner [17]. All the first-

order derivatives with respect to ξ are replaced by two-point backward difference formulae of the form

$$\partial H/\partial\xi = (H_{ij} - H_{i-i,j})/\Delta\xi, \tag{11}$$

where H represents dependent variable f or g and i and j are the node locations along ξ and η directions, respectively. First the third-order differential equation (6) is converted into second order by substituting $F = f'$. Then the second-order derivatives in the η direction for F and g are discretized using three-point central difference formulae while the first-order derivatives in the η direction are discretized by employing the trapezoidal rule. At each line of constant ξ, a system of algebraic equations is obtained. The non-linear terms are evaluated at the previous iteration and the system of algebraic equations is solved iteratively by using the Thomas algorithm (see [17]). The same procedure is repeated for next ξ value and the equations are solved line by line until the desired ξ value is reached. A convergence criterion based on the relative difference between the current and the previous iterations is used. When this difference reaches 10^{-5}, the solution is supposed to have converged and the iterative process is terminated.

The effect of the grid size $\Delta\eta$ and $\Delta\xi$ and the edge of the boundary layer η_∞ on the solutions is examined. The results presented here are independent of the grid size and η_∞ at least up to the 4th decimal place.

4. Results and discussion

In order to assess the accuracy of our method, we have compared our skin friction coefficient ($C_f\ Re_X^{1/2}$) and the mass (heat) transfer coefficient in terms of the Sherwood (Nusselt) number ($2\ Sh Re_x^{-1/2} = 2Nu Re_x^{-1/2}$) for $M = \beta = 0$, $Sc = 0.7$ with those of Jeng et al. [14]. It may be noted that Eq. (7) is the same as that of Jeng et al. [14] if we replace Sc by Pr and Sh by Nu. Also, for $M = \xi = 0$, $\lambda = \lambda_3 = 1$, we have compared our mass transfer ($Sh\ Re_x^{-1/2}$) with that of Andersson et al. [15] (see Table 1). In both the cases, the results are found to be in good agreement. However, for $\xi > 0.5$, the results slightly differ (about 4%) from those of Jeng et al. [14]. This difference is attributed to the series solution method (an approximate method) used by Jeng et al. Also for $\beta = 0.01$ and $Sc = 0.1$, the mass transfer results differ from those of Andersson et al. by about 5%.

The effect of the magnetic parameter on the surface sheer stress ($-f''(\xi,0)$) for $N = Sc = \beta = 1$, $0 \leqslant \xi \leqslant 1$ is presented in Fig. 2. The magnetic parameter M strongly affects $f''(\xi,0)$ and the effect becomes more pronounced with increasing ξ. For example, for $\xi = 0.1$, $-f''(\xi,0)$ increases by about 43% as M increases from zero to 4, but for $\xi = 1$ it increases by about 115%. This increase in $-f''(\xi,0)$ with M is due to the enhanced Lorentz force which imparts additional momentum in the boundary layer. Since M is associated with the function λ_1 which vanishes at $\xi = 0$ and increases with ξ, the effect of M becomes more pronounced with increasing ξ.

Fig. 3 shows the effect of magnetic parameter M on the surface mass transfer ($-g'(\xi,0)$) for $N = Sc = \beta = 1$, $0 \leqslant \xi \leqslant 1$. Since M does not occur explicity in the diffusion equation, its effect on the mass transfer ($-g'(\xi,0)$) is small. For example, for $\xi = 0.5$, $-g'(\xi,0)$ decreases by about 7% as M increases from zero to 4. However, the mass transfer ($-g'(\xi,0)$) for $M = 1$ increases by about

Table 1
Comparison of the surface mass transfer coefficient ($Sh\,Re_x^{-1/2}$) with that of Andersson et al. [15] for $\xi = 0, \lambda = \lambda_1 = \lambda_3 = 1$

β	Sc	Present results			Anderson et al. [15]		
		$N = 1$	$N = 2$	$N = 3$	$N = 1$	$N = 2$	$N = 3$
0.01	0.1	0.10306	0.10000	0.09857	0.0998	0.0959	0.0944
0.1	0.1	0.15042	0.13077	0.12143	0.149	0.129	0.118
1.0	0.1	0.34940	0.28738	0.25085	0.348	0.286	0.249
10.0	0.1	1.01816	0.83237	0.72107	1.017	0.831	0.720
0.01	1.0	0.59216	0.58844	0.58682	0.592	0.588	0.587
0.1	1.0	0.67044	0.63724	0.62314	0.669	0.636	0.622
1.0	1.0	1.17761	1.00100	0.90765	1.177	1.000	0.907
10.0	1.0	3.23257	2.64963	2.30414	3.232	2.649	2.303
0.01	10	2.33011	2.32230	2.31949	2.334	2.327	2.324
0.1	10	2.50402	2.43573	2.40463	2.509	2.440	2.409
1.0	10	3.87469	3.39719	3.15387	3.880	3.400	3.157
10.0	10	10.24283	8.41668	7.35074	10.25	8.418	7.352
0.01	100	7.82788	7.80869	7.79944	7.886	7.870	7.861
0.1	100	8.33179	8.14180	8.05203	8.395	8.202	8.112
1.0	100	12.44321	11.01630	10.29294	12.51	11.07	10.35
10.0	100	32.41681	26.66513	23.32715	32.47	26.70	23.36

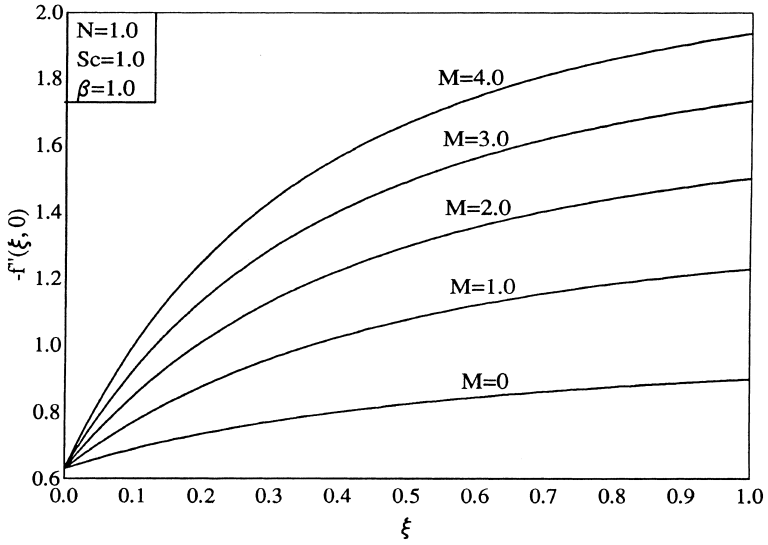

Fig. 2. Effect of the magnetic parameter M on the surface shear stress $(-f''(\xi, 0))$.

106% as ξ increases from zero to 1, since the concentration boundary layer becomes thin with increasing values of ξ.

Fig. 4 displays the effect of Schmidt number (Sc) on the surface mass transfer $(-g'(\xi, 0))$ for $N = \beta = M = 1$, $0 \leqslant \xi \leqslant 1$. The surface mass transfer strongly depends on Sc, since it occurs explicitly in the diffusion equation. The mass transfer increases by about 167% as Sc increases from

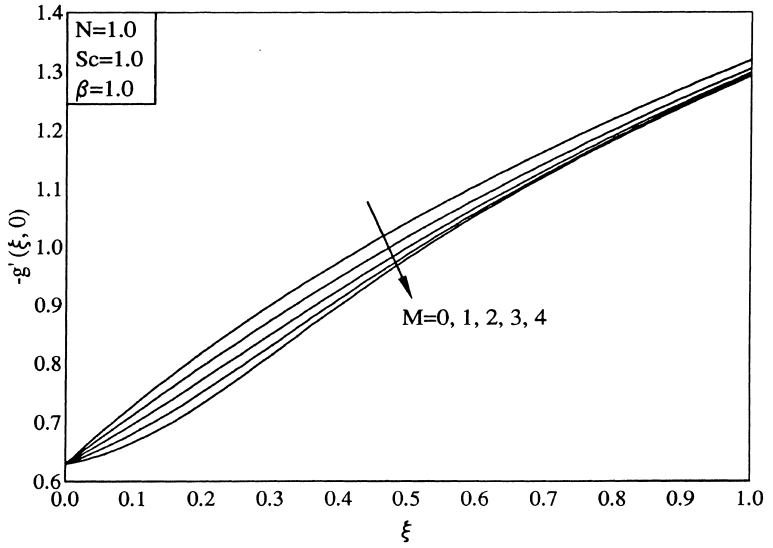

Fig. 3. Effect of the magnetic parameter M on the surface mass transfer $(-g'(\xi,0))$.

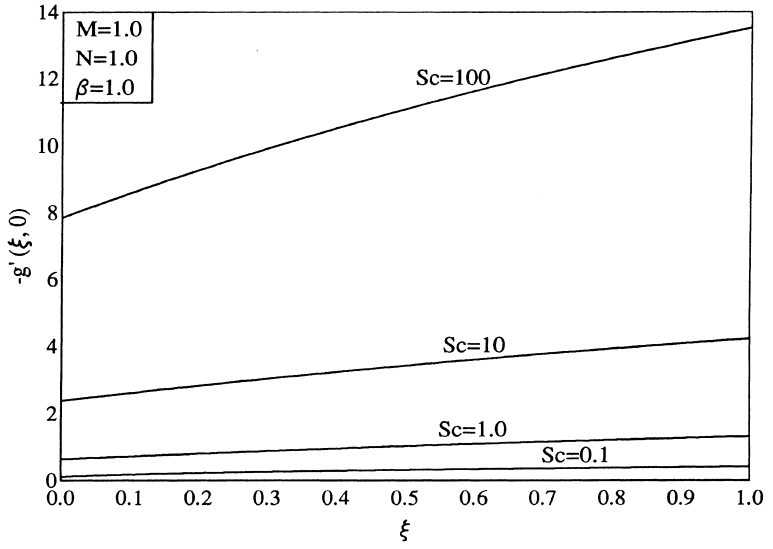

Fig. 4. Effect of the Schmidt number Sc on the surface mass transfer $(-g'(\xi,0))$.

1 to 10 when $\xi = 1$. The reason for this trend is that the concentration boundary layer becomes thin for large Sc. For small Sc, $g'(\xi,0)$ changes little with ξ.

The effect of the reaction rate parameter β on the surface mass transfer $(-g'(\xi,0))$ for $M = N = Sc = 1$ is shown in Fig. 5. The surface mass transfer is strongly affected by β. For $\xi = 1$, it increases by about 450% as β increases from zero to 5. This increase in $-g'(\xi,0)$ is caused by a large reduction in the concentration boundary layer thickness.

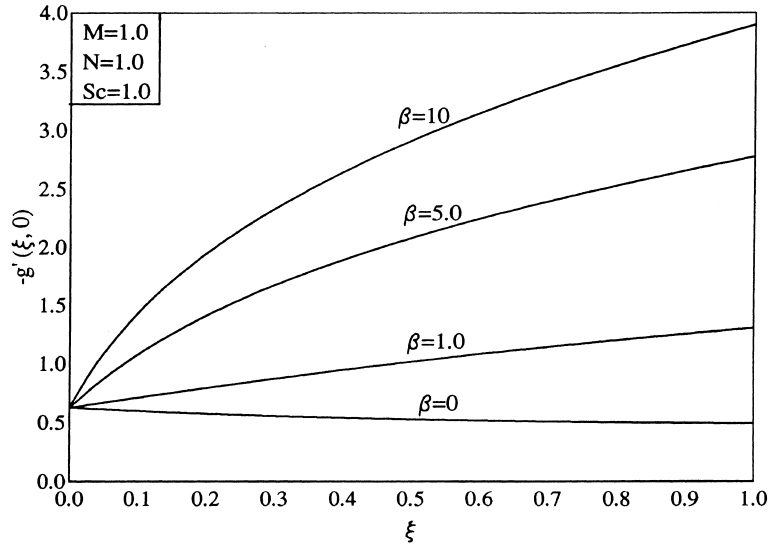

Fig. 5. Effect of reaction rate β on the surface mass transfer $(g'(\xi,0))$.

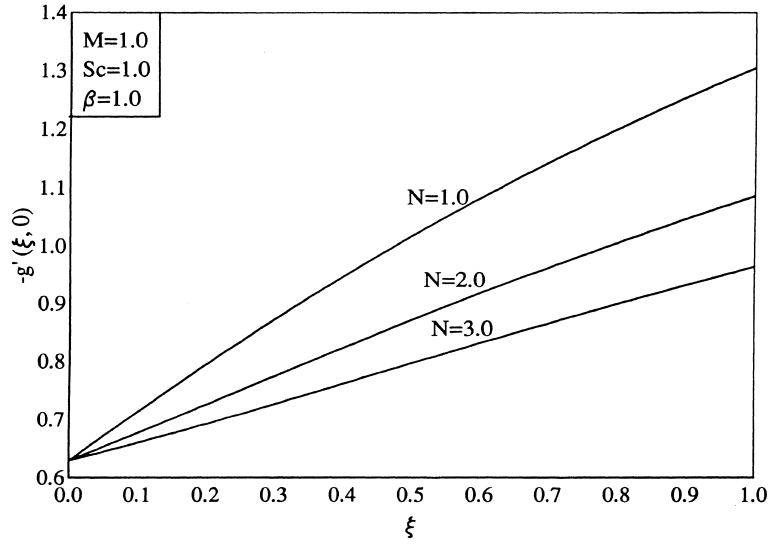

Fig. 6. Effect of the order of reaction N on the surface mass transfer $(g'(\xi,0))$.

Fig. 6 presents the effect of the order of reaction N on the surface mass transfer $(-g'(\xi,0))$ for $M = Sc = \beta = 1$, $0 \leqslant \xi \leqslant 1$. The interesting result is that the surface mass transfer decreases for higher-order reaction. At $\xi = 1$, it decreases by about 27% as N increases from 1 to 3.

The effect of M on the velocity and concentration profiles $(f'(\xi,\eta), g(\xi,\eta))$ for $N = Sc = \beta = 1, \xi = 0.5$ is presented in Fig. 7. The velocity boundary layer becomes thin as M increases, but concentration boundary layer becomes thick. Hence velocity profiles become more steep with increasing M, but concentration profiles become less steep. In the presence of the

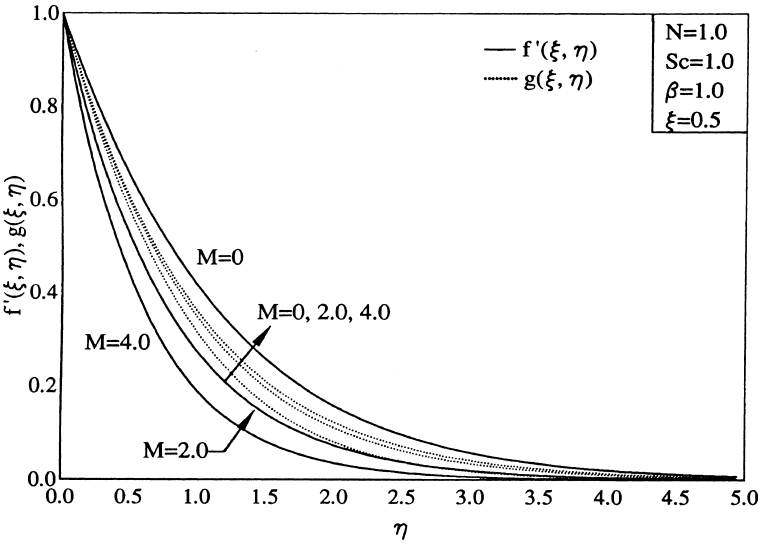

Fig. 7. Effect of the magnetic parameter M on the velocity and concentration profiles $(f'(\xi,\eta), g(\xi,\eta))$.

magnetic field, the velocity boundary layer is thinner than the concentration boundary layer, but for $M = 0$ an opposite trend is observed.

The effects of the Schmidt number (Sc), reaction rate (β), order of reaction (N) and the streamwise distance ξ on the concentration profiles ($g(\xi,\eta)$) are, respectively, shown in Figs. 8–11. The concentration boundary layer becomes thin as Sc or β or ξ increases, but grows with N. Hence concentration decreases with an increase in Sc, β and ξ, but increases as N increases.

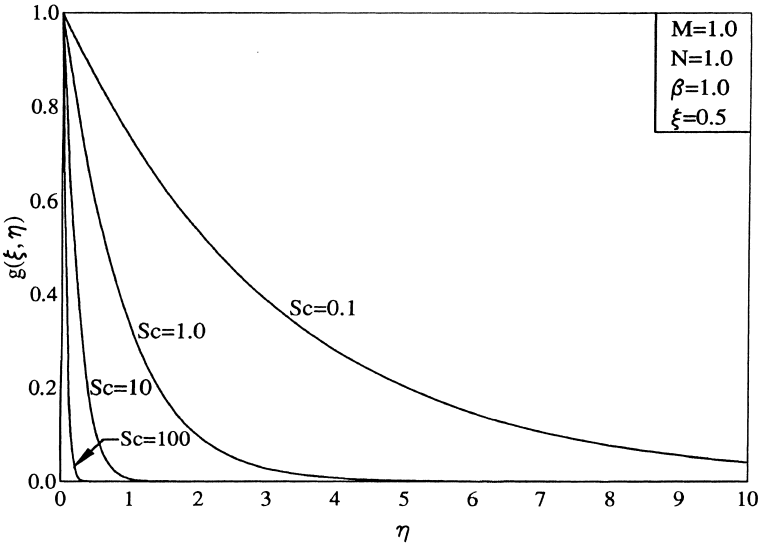

Fig. 8. Effect of the Schmidt number Sc on the concentration profiles $(g(\xi,\eta))$.

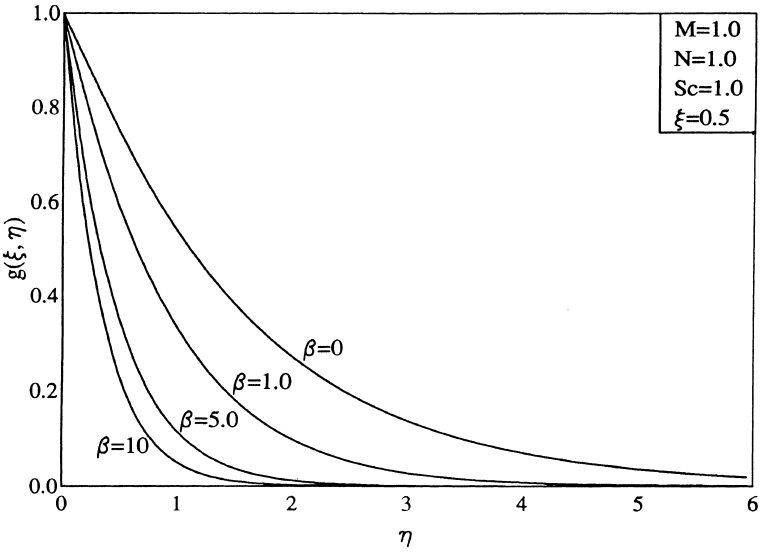

Fig. 9. Effect of the reaction rate parameter β on the concentration profiles ($g(\xi,\eta)$).

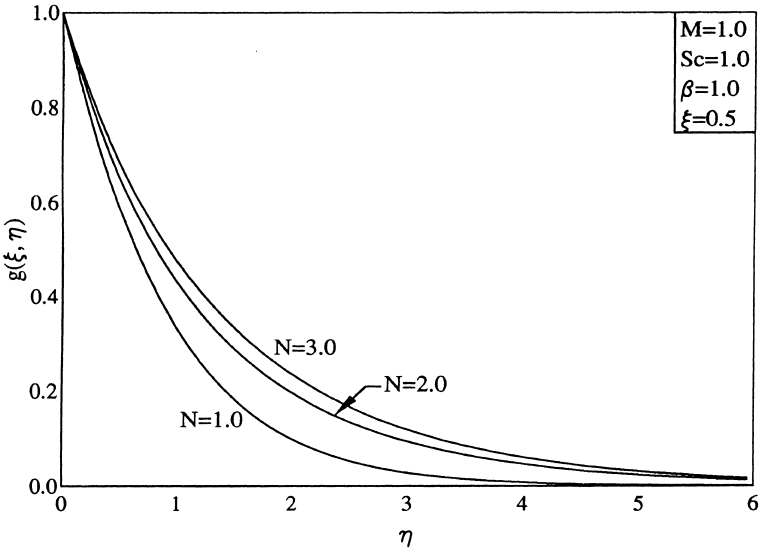

Fig. 10. Effect of the order of reaction β on the concentration profiles ($g(\xi,\eta)$).

5. Conclusions

An important result is that the surface skin friction is significantly increased by the magnetic field, but the surface mass transfer is slightly reduced. The effect of the magnetic field on the skin friction becomes more pronounced as the streamwise distance increases. Another important result is that the surface mass transfer for the first order reaction is more than that of the second or

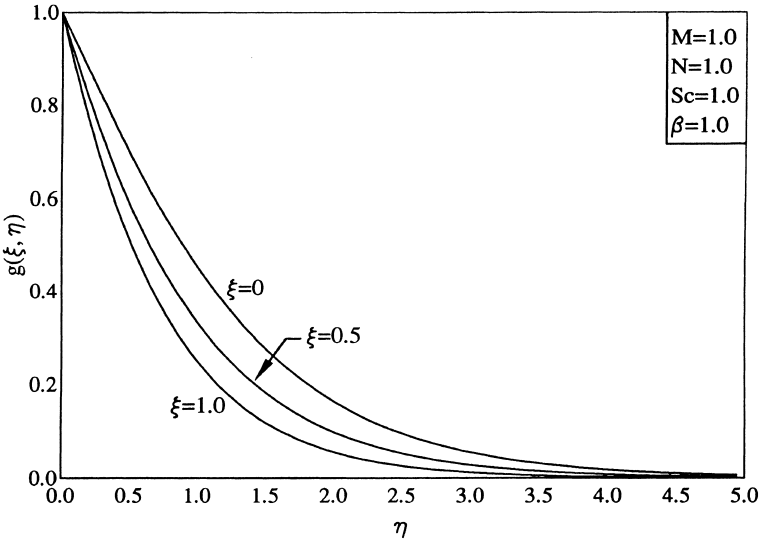

Fig. 11. Effect of the streamwise distance ξ on the concentration profiles ($g(\xi,\eta)$).

higher order reaction. The surface mass transfer strongly depends on the Schmidt number and the reaction rate and it increases with their increasing values. Further, the surface mass transfer increases significantly with the streamwise distance for higher values of the Schmidt number and the reaction rate. However, for higher-order reaction, an opposite trend is observed. The velocity decreases with increasing magnetic fields, but concentration slightly increases. Also, the concentration decreases with increasing Schmidt number, the reaction rate and the streamwise distance, but it increases as the order of reaction increases.

References

[1] R.M. Griffith, Velocity temperature and concentration distributions during fibre spinning, Ind. Eng. Chem. Fundam. 3 (1964) 245–250.
[2] L.E. Erickson, L.T. Fan, V.G. Fox, Heat and mass transfer on a moving continuous flat plate with suction or injection, Ind. Eng. Chem. Fundam. 5 (1966) 19–25.
[3] D.T. Chin, Mass transfer to a continuous moving sheet electrode, J. Electrochem. Soc. 122 (1975) 643–646.
[4] R.S.R. Gorla, Unsteady mass transfer in the boundary layer on a continuous moving sheet electrode, J. Elecrochem. Soc. 125 (1978) 865–869.
[5] L.J. Crane, Flow past a stretching plate, Z. Angew Math. Phys. 21 (1970) 645–647.
[6] J. Vleggaar, Laminar boundary layer behaviour on continuous accelarating surfaces, Chem. Eng. Sci. 32 (1977) 1517–1525.
[7] P.S. Gupta, A.S. Gupta, Heat and mass transfer on a stretching sheet with suction or blowing, Can. J. Chem. Eng. 55 (1977) 744–746.
[8] A. Chakrabarti, A.S. Gupta, Hydromagnetic flow heat and mass transfer over a stretching sheet, Quart. Appl. Math. 33 (1979) 73–78.
[9] P. Carragher, L.J. Crane, Heat transfer on continous stretching sheet, Z. Angew. Math. Mech. 62 (1982) 564–565.
[10] L.J. Grubka, K.M. Bobba, Heat transfer characteristics of a continuous stretching surface with variable temperature, J. Heat Transfer 107 (1985) 248–250.

[11] C.K. Chen, M.J. Char, Heat transfer of a continuous stretching surface with suction or blowing, J. Math. Anal. Appl. 135 (1988) 568–580.
[12] B.K. Dutta, Heat transfer from a stretching sheet with uniform suction or blowing, Acta Mechanica 78 (1989) 255–262.
[13] H.I. Andersson, An exact solution of the Navier–Stokes equations for MHD flow, Acta Mechanica 113 (1995) 241–244.
[14] D.R. Jeng, T.C.A. Chang, K.J. De Witt, Momentum and heat transfer on a continuous moving surface, ASME J. Heat Transfer 108 (1986) 532–539.
[15] H.I. Andersson, O.R. Hansen, B. Holmedal, Diffusion of a chemically reactive species from a stretching sheet, Int. J. Heat Mass Transfer 37 (1994) 659–664.
[16] A.C. Eringen, G.A. Maugin, Electrodynamics of Continua II, Springer, Berlin, 1990.
[17] F.G. Blottner, Finite-difference methods of solution of the boundary layer equations, AIAA. J. 8 (1970) 193–205.